Numerical Modelling of Terahertz Systems for Nondestructive Evaluation of Dielectric Materials

Przemysław Lopato, Tomasz Chady, Ryszard Sikora, Stanislaw Gratkowski, Marcin Ziolkowski

West Pomeranian University of Technology

Department of Electrical and Computer Engineering

ul. Sikorskiego 37, 70-313 Szczecin

POLAND

Zachodniopomorski Uniwersytet Technologiczny w Szczecinie

This work was supported in part by the State Committee for Scientific Research, Poland under Grant (N N510 538039) “Nondestructive testing of composite materials using terahertz frequency electromagnetic waves” (2010-2013)

Presentation outline

1. **Introduction to pulsed THz imaging**
2. **THz imaging system description**
3. **Frequency domain FEM analysis**
4. **Time domain FDTD analysis**
5. **Conclusions**

Introduction to pulsed THz imaging

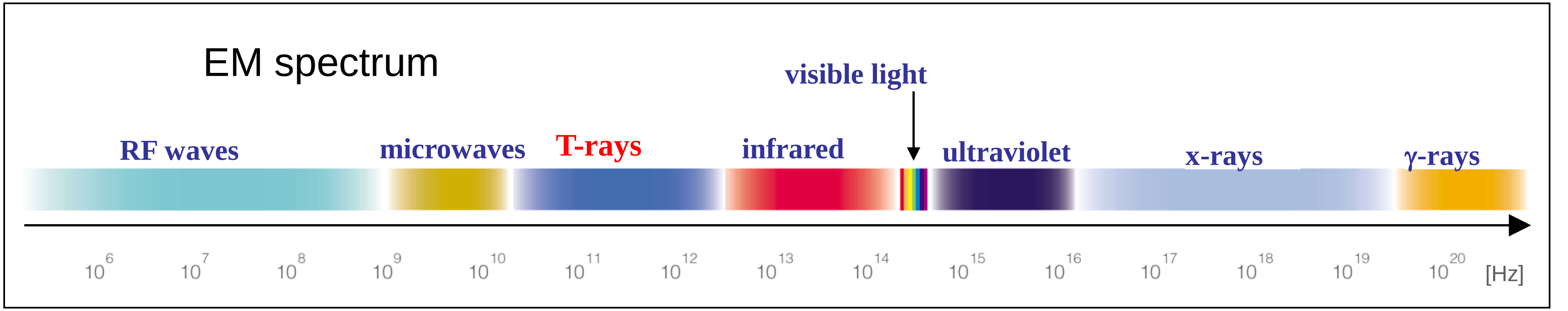

Terahertz electromagnetic radiation enables non-invasive, non-ionizing and non-contact examination of dielectric materials such as: plastics, dry wood, explosives ceramics, foams and composites - especially glass fiber reinforced. The T-Rays are sensitive for refractive index. Any defect which disturbs refractive index can be detected , e.g.:

- void,
- delamination,
- inclusion,
- material inhomogeneities (fiber/matrix distribution),
- surface roughness,
- fiber waviness,
- internal interfaces between layers (in layered structures).

Introduction to pulsed THz imaging

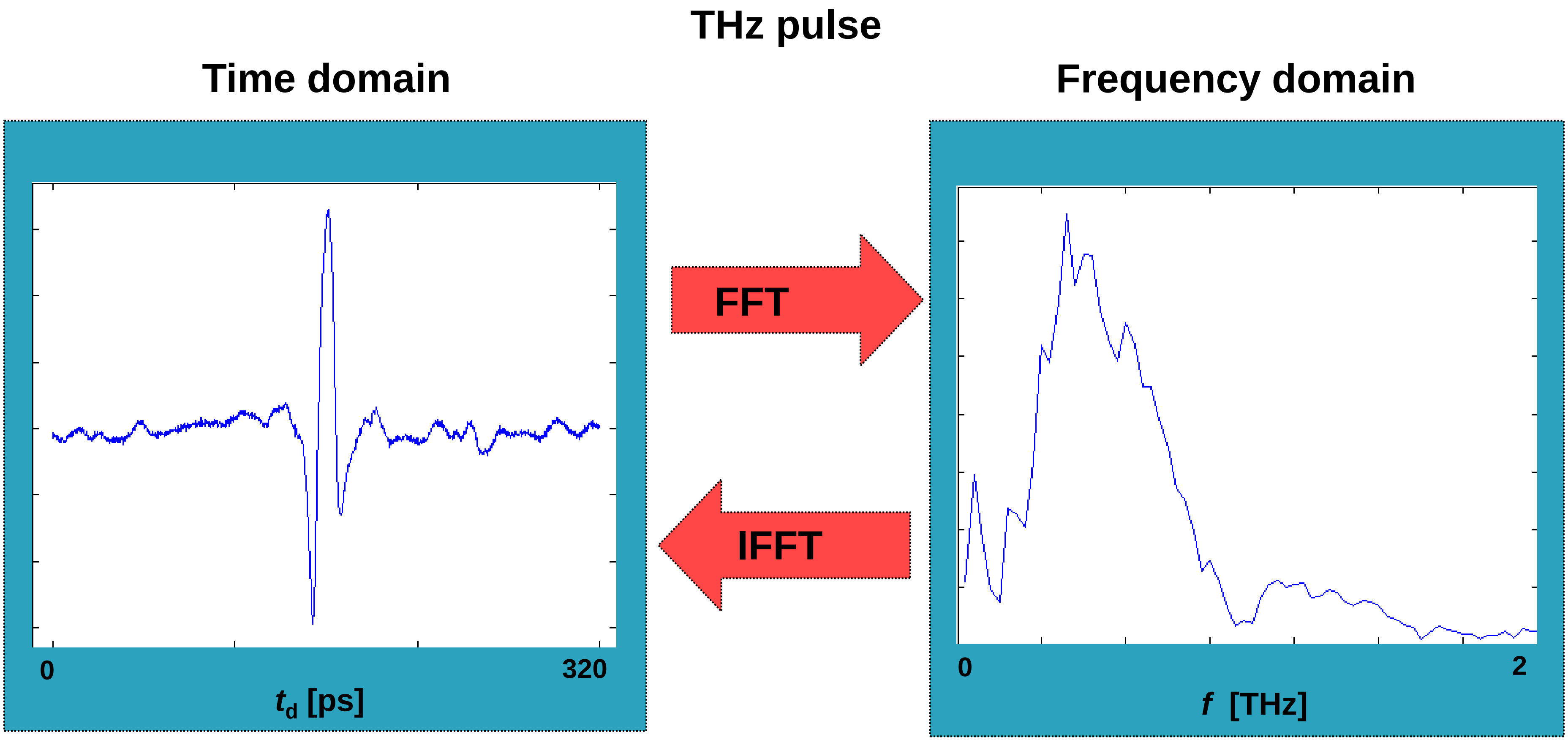

THz imaging system description

Simplified scheme of the measuring system

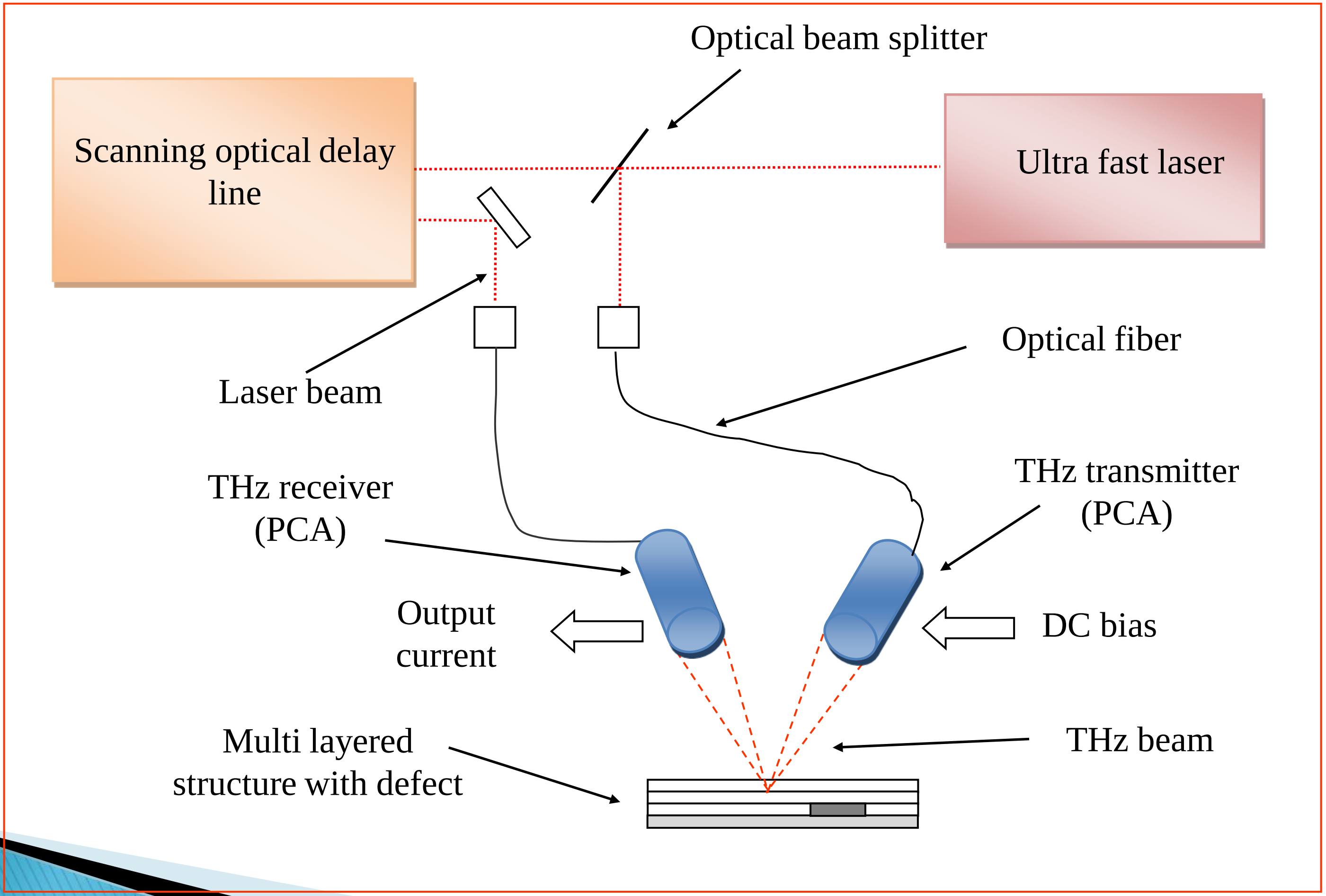

THz imaging system description

View of a modelled pulsed THz inspection system

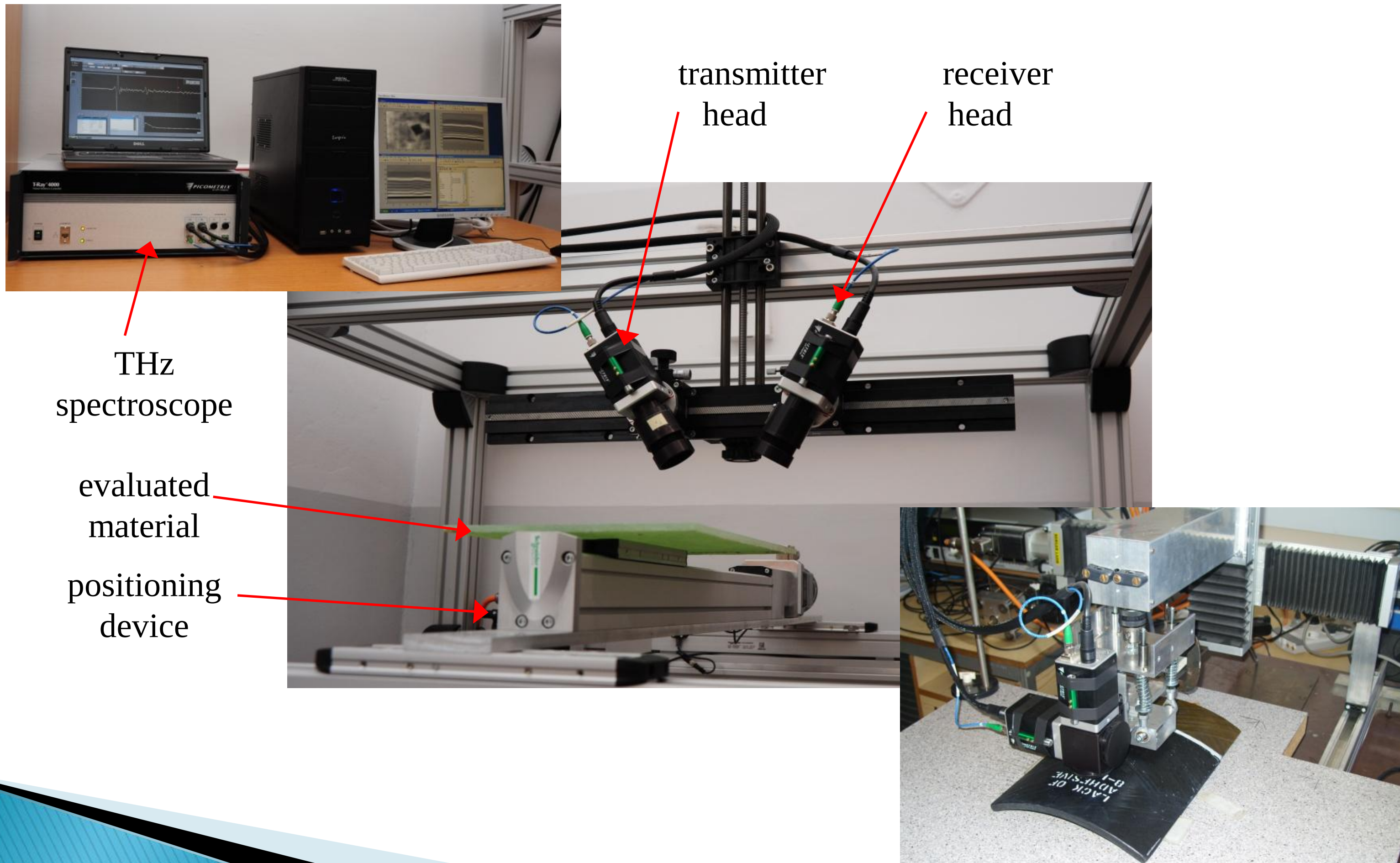

THz imaging system description

Terahertz frequency EM waves are excited with Photo Conductive Antennas (PCA)

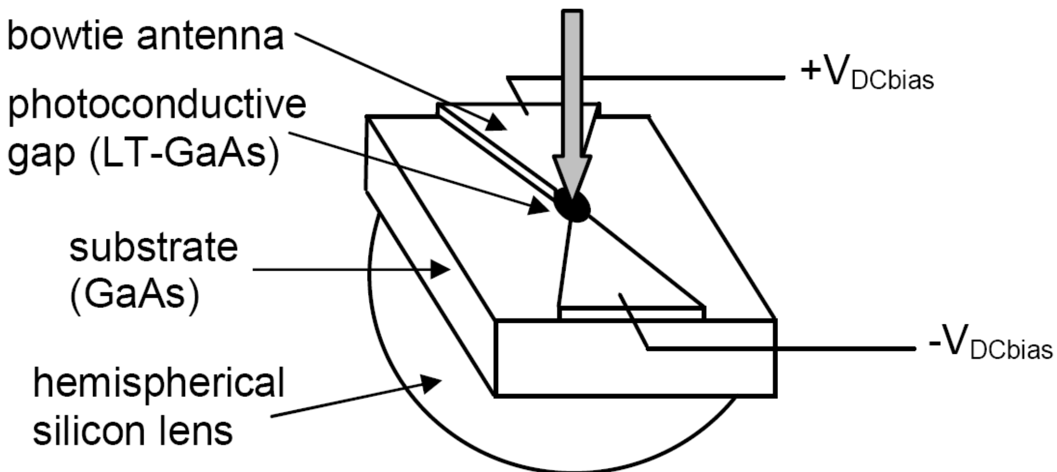

Photo Conductive Antenna - (Picometrix, USA)

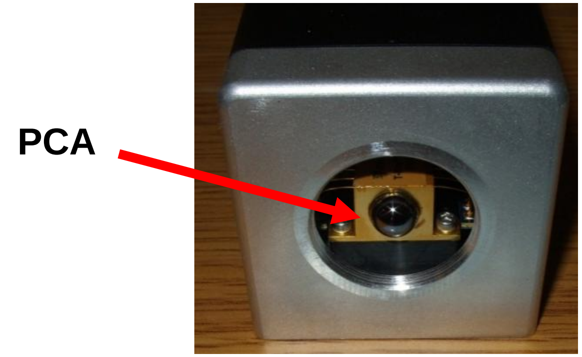

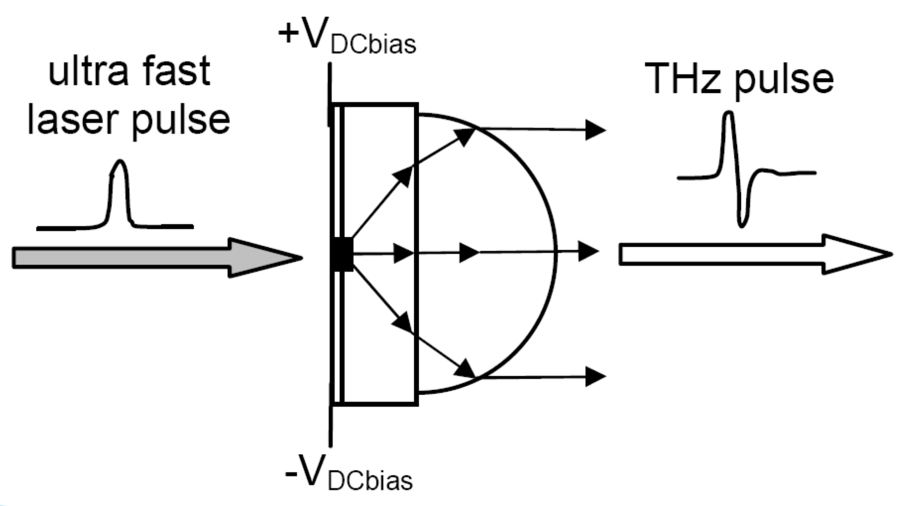

Numerical model geometry

Designing the optimum geometry of the terahertz measurement systems and estimating the efficiency of existing and newly developed algorithms for reconstruction of the inner structure of the examined material requires the use of appropriate numerical modelling. In order to simulate the operation of the THz devices or the propagation of electromagnetic terahertz waves, full-wave methods (e.g. finite element method – FEM, finite difference time domain method – FDTD) and algorithms based on high frequency approximation (e.g. ray tracing) are used.

Wavelengths (fraction of millimeter) corresponding to terahertz pulses propagating in a dielectric medium are several orders of magnitude smaller than the dimensions of the measuring system geometry (tens of centimeters). This causes that the use of full-wave numerical methods like FEM or FDTD, is applicable only in case of two-dimensional modelling. In following sections we present frequency domain analysis using FEM, and then the results of time domain FDTD simulations are shown.

Numerical model geometry

The main computation area consists of:

- air environment,
- transmitting/receiving PCA antenna,
- HDPE focusing lens,
- evaluated material with defect (here: air inclusion).

The dimensions of analysed geometry agree with real ones. No dispersion and absorption effects were taken into account in our simplified model. We assumed that a single PCA is both: transmitter and receiver.

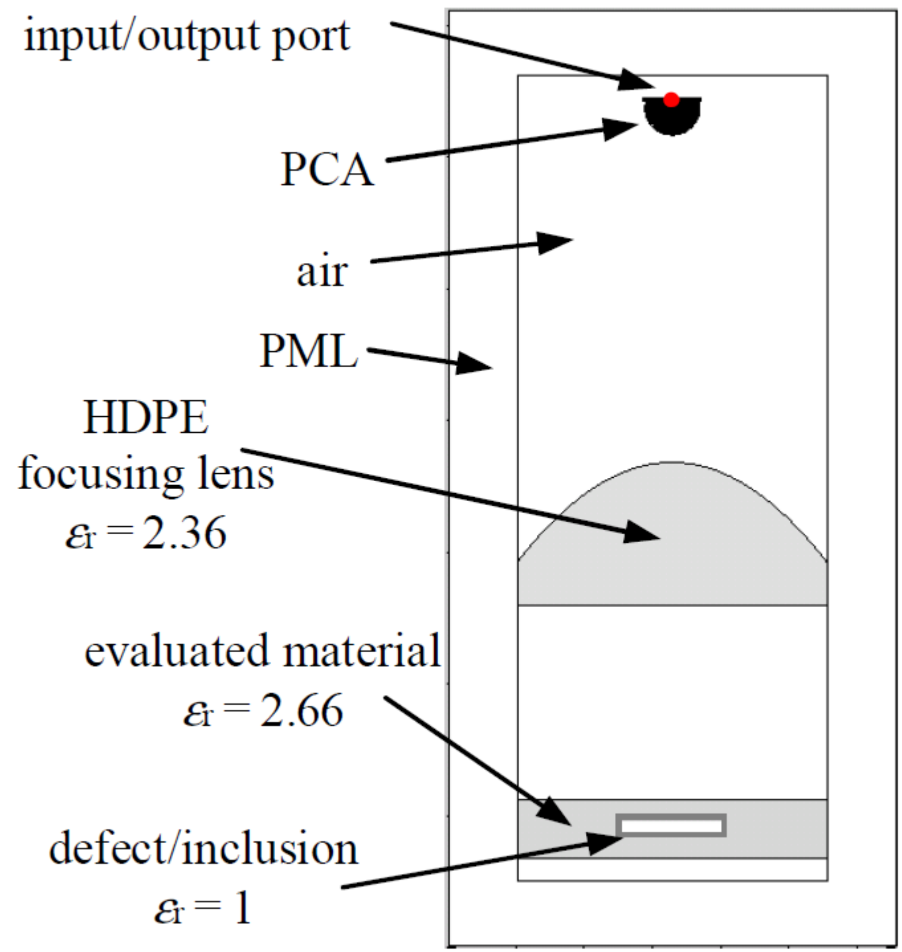

Frequency Domain FEM Analysis

Mathematical models for high-frequency electromagnetic waves are based on Maxwell-Ampère's and Faraday's laws:

$$\nabla \times \boldsymbol{H} = \boldsymbol{J} + \frac{\partial \boldsymbol{D}}{\partial t}$$

$$\nabla \times \boldsymbol{E} = -\frac{\partial \boldsymbol{B}}{\partial t}$$

where: ***H***, ***B*** and ***E***, ***D*** are the magnetic and electric vectors at time *t*, ***J*** is the current density vector.

Frequency Domain FEM Analysis

Using the constitutive relations for linear materials $\boldsymbol{B} = \mu\boldsymbol{H}$ and $\boldsymbol{D} = \varepsilon\boldsymbol{E}$ as well as the expression for current density $\boldsymbol{J} = \boldsymbol{J}_s + \sigma\boldsymbol{E}$ (μ, ε and σ are the magnetic permeability, electric permittivity and conductivity, respectively, $\boldsymbol{J}_s$ is the source current density vector), after some manipulations, we have the following equation for the electric vector:

$$\nabla \times \left(\nabla \times \boldsymbol{E}\right) = -\mu \frac{\partial \boldsymbol{J}_\mathrm{s}}{\partial t} - \sigma\mu \frac{\partial \boldsymbol{E}}{\partial t} - \varepsilon\mu \frac{\partial^2 \boldsymbol{E}}{\partial t^2}$$

Assuming harmonic time dependence the equation becomes:

$$\text{(1)} \qquad \nabla \times \left(\nabla \times \underline{\boldsymbol{E}}\right) = -\mathrm{j}\omega\mu\underline{\boldsymbol{J}}_\mathrm{s} + \omega^2\mu\underline{\varepsilon}_\mathrm{e}\underline{\boldsymbol{E}} \quad , \quad \underline{\varepsilon}_\mathrm{e} = \varepsilon - \mathrm{j}\sigma/\omega$$

Frequency Domain FEM Analysis

- One of the major challenges in the finite element analysis of high-frequency electromagnetic problems is the truncation of unbounded space into a finite computational domain.
- On the artificial boundary suitable boundary conditions must be imposed to simulate the extension of the solution region to infinity.
- Different approaches can be found in the literature (infinite elements, perfectly matched layers – PMLs, approximate boundary conditions).
- In this section we used so called absorbing boundary conditions – ABCs.
- The ideal boundary conditions should make the artificial boundary completely transparent to the radiated field, such that the radiated field can pass through it without any distortion or reflection.
- This is not possible in practice. For that reason we employ approximate ABCs. ABCs of different order can be formulated using the general form of the solution to Helmholtz's equation (1).

Frequency Domain FEM Analysis

For example, for the 2D wave equation, $\underline{\mathbf{E}} = \underline{E}_z(r, \varphi)\,\mathbf{1}_z$, in cylindrical polar co-ordinates an asymptotic expression for $\underline{E}_z(r, \varphi)$ can be written at large distance from the origin as follows:

$$\underline{E}_z(r,\varphi) \approx \frac{e^{-jkr}}{\sqrt{r}}\left[A_0(\varphi) + \frac{A_1(\varphi)}{r} + \frac{A_2(\varphi)}{r^2} + \ldots\right] \quad , \quad k = \omega\sqrt{\varepsilon\mu} \tag{2}$$

It can be easily shown that manipulation of the general solution (2) leads to the following boundary conditions on a circular artificial boundary of radius r :

$$\frac{\partial \underline{E}_z}{\partial r} + jk\underline{E}_z + \frac{\underline{E}_z}{2r} = O\left(r^{-5/2}\right) \tag{3}$$

which is recognized as the first-order ABC, and

$$\frac{\partial^2 \underline{E}_z}{\partial r^2} + \frac{3}{r}\frac{\partial \underline{E}_z}{\partial r} + \frac{3}{4r^2}\underline{E}_z + 2jk\frac{\partial \underline{E}_z}{\partial r} + \left(\frac{3jk}{r} - k^2\right)\underline{E}_z = O\left(r^{-9/2}\right) \tag{4}$$

- the second-order ABC

Frequency Domain FEM Analysis

The conditions (3) and (4) can be transferred for rectangular boundaries in the *x*-*y* plane. An implementation of ABCs in FEM program is straightforward when the code of the program is available. Unfortunately, it is not the case when we are using commercial software. Fortunately, for *RF COMSOL Multiphysics* module it is enough to choose so called *surface current* boundary conditions ($-\boldsymbol{n} \times \boldsymbol{H} = \boldsymbol{J}_s$), which can be found in the boundary conditions section.

1st order ABC, *x* = const

$$-\boldsymbol{n}\times\boldsymbol{H} = \frac{1}{j\omega\mu}\left[\frac{y}{x}\frac{\partial \underline{E}_z}{\partial y} + \left(jk\sqrt{1+\left(y/x\right)^2} + \frac{1}{2x}\right)\underline{E}_z\right]1_z \qquad (5)$$

2nd order ABC, *x* = const

$$-\boldsymbol{n}\times\boldsymbol{H} = \frac{1}{j\omega\mu\frac{x}{r}\left(\frac{3}{r}+2jk\right)}\left[-\frac{\partial^2 \underline{E}_z}{\partial y^2} - \left(\frac{k^2x^2}{r^2} + k^2 + \frac{2jky^2}{r^3} - \frac{3jk}{r} - \frac{3}{4r^2}\right)\underline{E}_z\right],\ r=\sqrt{x^2+y^2} \qquad (6)$$

Frequency Domain FEM Analysis

For y = const it is enough to change coordinate x with y. In fact, in derivation of the boundary condition (6) we have used the first-order ABC (5) to approximate the term $\partial^2\underline{E}_z/\partial x\partial y$.

The model from Fig. 4 has been calculated using *COMSOL Multiphysics RF* module with the boundary condition (6) on the outer artificial boundaries. It was assumed 10 finite triangular elements per wavelength (frequency of the electromagnetic wave f = 0.1 THz). The total number of finite elements was equal to 225 640.

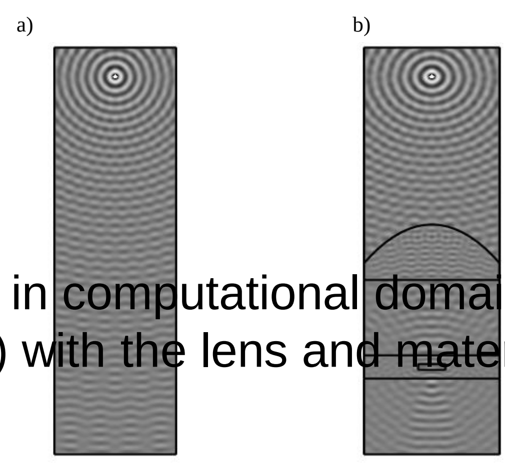

Normalized E_z distribution in computational domain: a) without focusing lens and material under test, b) with the lens and material under test in place.

Time Domain FDTD Analysis

Modeled measurement system in its operating principle uses pulses of electromagnetic field. Therefore, the FDTD method (working in time domain) seems to be a natural solution of the forward problem.
In this model, a Transverse Magnetic (TM) mode and PML absorbing boundary conditions were used. In two dimensional Cartesian coordinate system and TM mode, only electric *Ez and magnetic Hx, Hy* field components exist, thus Maxwell equations become:

$$\varepsilon \frac{\partial E_z}{\partial t} = \frac{\partial H_y}{\partial x} - \frac{\partial H_x}{\partial y} - \sigma E_z$$

$$\mu \frac{\partial H_x}{\partial t} = -\frac{\partial E_z}{\partial y} \qquad (7)$$

$$\mu \frac{\partial H_y}{\partial t} = \frac{\partial E_z}{\partial x}.$$

Time Domain FDTD Analysis

This system of equations discretized in time domain and in space using central difference approximation, may be written as:

$$\varepsilon_{i,j}\frac{E_z\big|_{i,j}^{n+0.5}-E_z\big|_{i,j}^{n-0.5}}{\Delta t}=\frac{H_y\big|_{i+0.5,j}^{n}-H_y\big|_{i-0.5,j}^{n}}{\Delta x}-\frac{H_x\big|_{i,j+0.5}^{n}-H_x\big|_{i,j-0.5}^{n}}{\Delta y}-\sigma_{i,j}\frac{E_z\big|_{i,j}^{n+0.5}+E_z\big|_{i,j}^{n-0.5}}{2}$$

(8)

$$\mu_{i,j+0.5}\frac{H_x\big|_{i,j+0.5}^{n+1}-H_x\big|_{i,j+0.5}^{n}}{\Delta t}=-\frac{E_z\big|_{i,j+1}^{n+0.5}-E_z\big|_{i,j}^{n+0.5}}{\Delta y}$$

$$\mu_{i+0.5,j}\frac{H_y\big|_{i+0.5,j}^{n+1}-H_y\big|_{i+0.5,j}^{n}}{\Delta t}=\frac{E_z\big|_{i+1,j}^{n+0.5}-E_z\big|_{i,j}^{n+0.5}}{\Delta x}$$

Time Domain FDTD Analysis

On the basis of difference equations the most actual *E*z, *H*x and *H*y field components are calculated and have the following form:

$$E_z\Big|_{i,j}^{n+0.5} = \frac{2\varepsilon_{i,j} - \Delta t \sigma_{i,j}}{2\varepsilon_{i,j} + \Delta t \sigma_{i,j}} E_z\Big|_{i,j}^{n-0.5} + \frac{2\Delta t}{2\varepsilon_{i,j} + \Delta t \sigma_{i,j}} \cdot \left[\frac{H_y\big|_{i+0.5,j}^{n} - H_y\big|_{i-0.5,j}^{n}}{\Delta x} - \frac{H_x\big|_{i,j+0.5}^{n} - H_x\big|_{i,j-0.5}^{n}}{\Delta y} \right]$$

(9)

$$H_x\Big|_{i,j+0.5}^{n+1} = H_x\Big|_{i,j+0.5}^{n} - \frac{\Delta t}{\mu_{i,j+0.5}\Delta y}\left[E_z\Big|_{i,j+1}^{n+0.5} - E_z\Big|_{i,j}^{n+0.5} \right]$$

$$H_y\Big|_{i+0.5,j}^{n+1} = H_y\Big|_{i+0.5,j}^{n} + \frac{\Delta t}{\mu_{i+0.5,j}\Delta x}\left[E_z\Big|_{i+1,j}^{n+0.5} - E_z\Big|_{i,j}^{n+0.5} \right]$$

Equations (9) are used to update field components in each time step.

Time Domain FDTD Analysis

Utilized orthogonal mesh consists of 1424×654 cells corresponding to 12.5×5.7 (cm) area. The total number of FDTD cells was equal to 931296. Space discretization step (cell size) is assumed to be the same in both *x*,*y* directions:

(10)
$$\Delta x = \Delta y = \frac{\lambda_{\mathrm{MIN}}}{10}$$

where:
λ_{MIN} – the shortest wavelength in computational domain.

Cell size utilized during computations was calculated as Δx=88.2 (μm). Time step length Δt=147 (fs) was estimated based on following equation:

(11)
$$\Delta t = \frac{\Delta x}{2c_0}$$

where:
c_0 – speed of light in free space.
Response for 6000 time steps were calculated during simulation. That corresponds to t = 882 (ps) of pulse travel time.

Time Domain FDTD Analysis

Calculated distribution of *Ez* field in computational domain is presented in case of four time points:
a) pulse is propagating through focusing lens,
b) focused pulse is approaching to materials surface,
c) pulse is propagating through an evaluated material and part of it is reflected back,
d) reflected pulses are approaching to PCA.

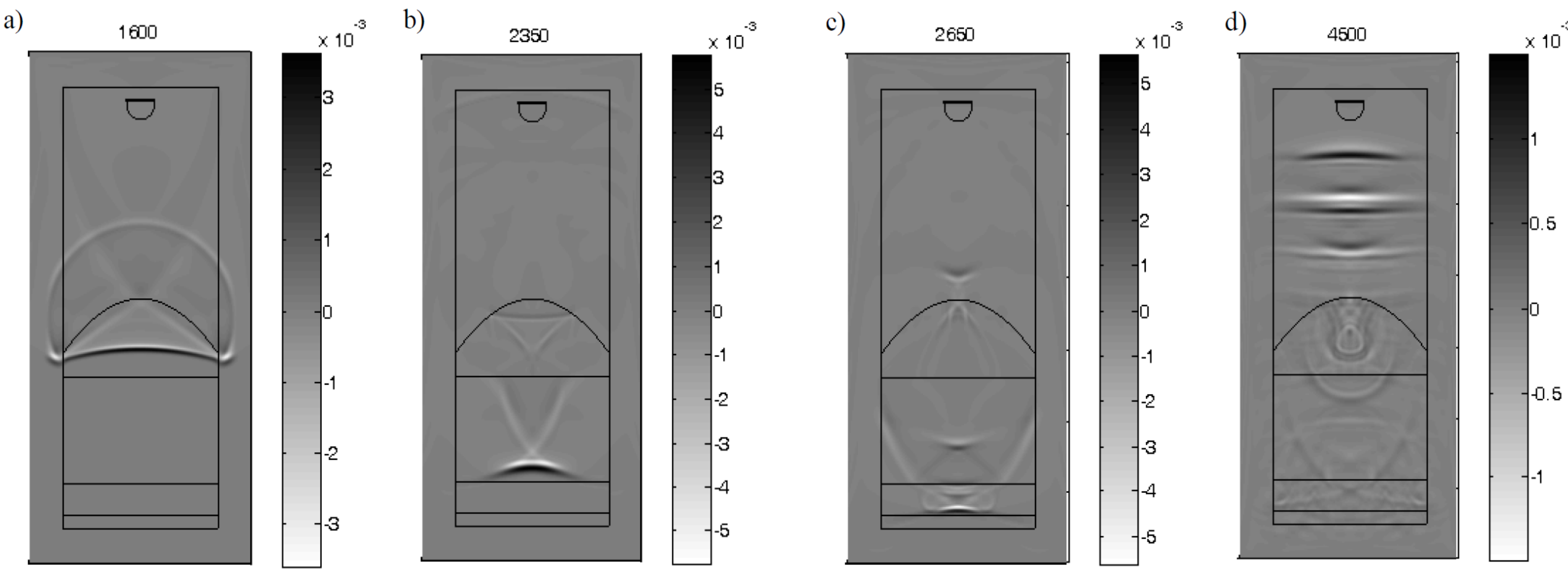

Time Domain FDTD Analysis

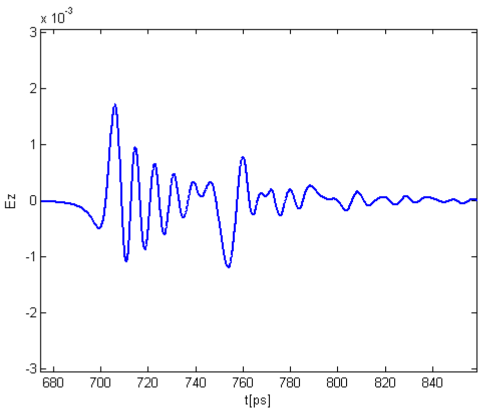

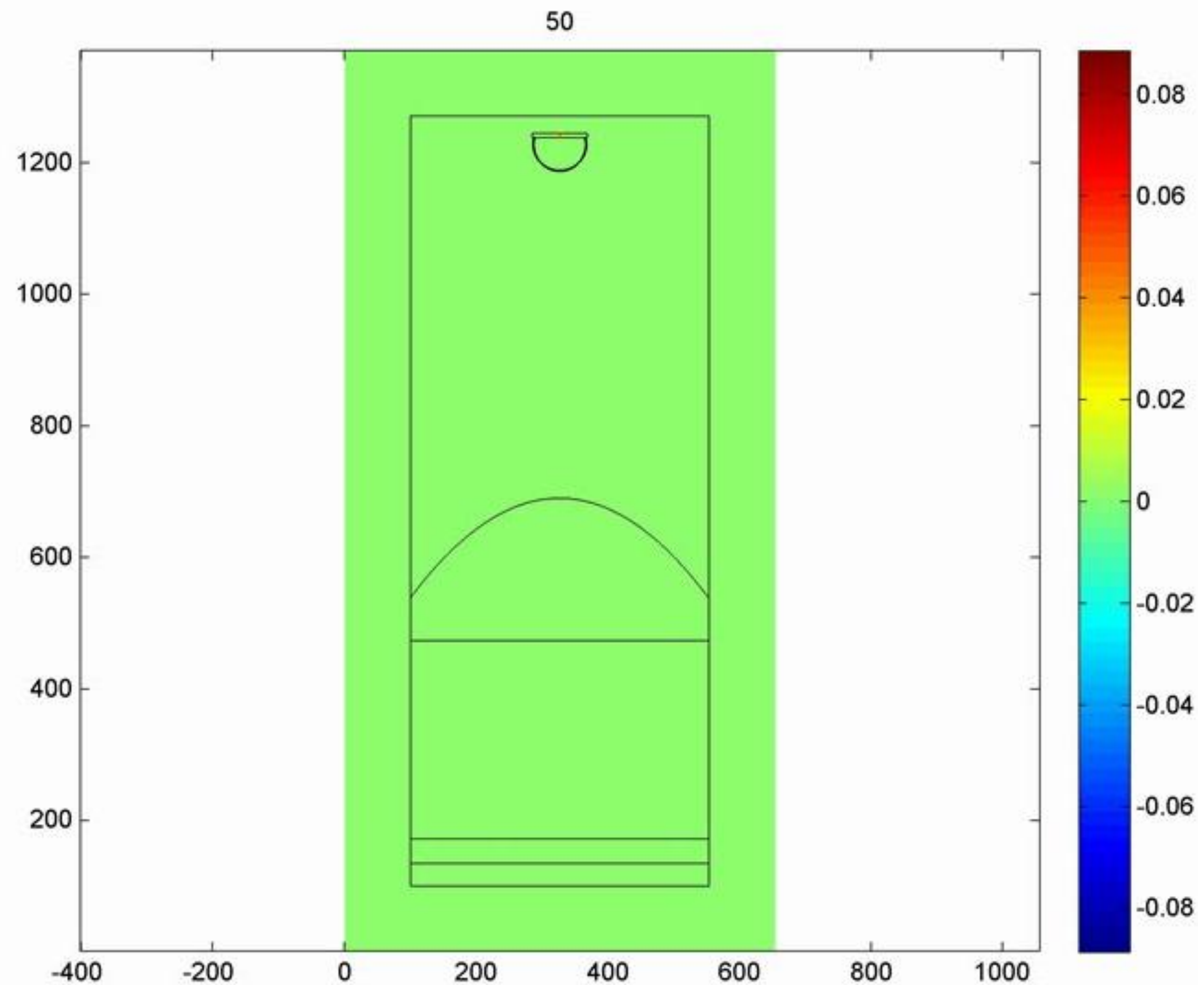

Time Domain FDTD Analysis

Obtained A-scan signals and their frequency spectrum in case of homogeneous and defected material (polymethyl methacrylate, PMMA)

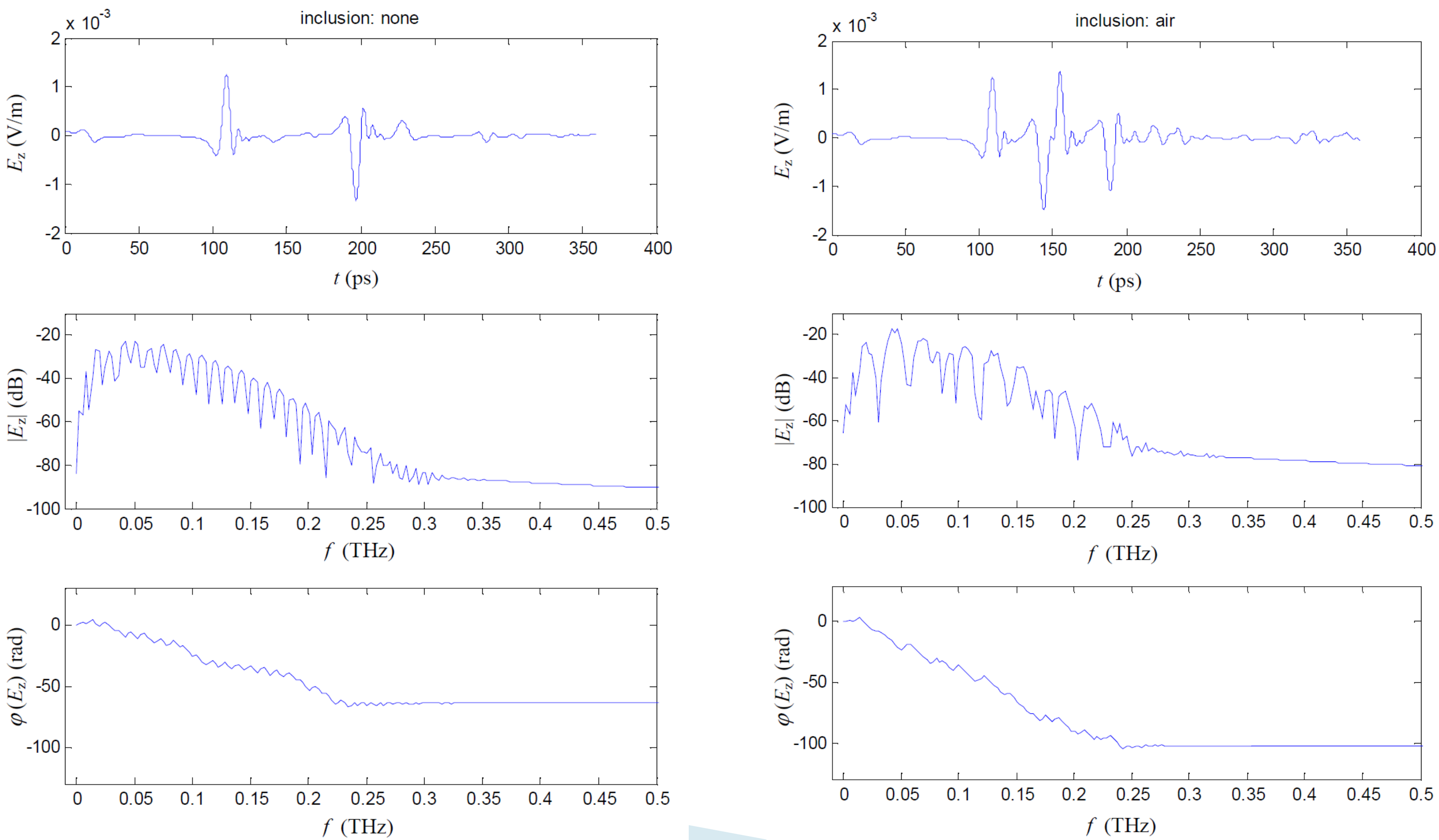

Time Domain FDTD Analysis

Comparison of simulated and measured A-scan signals

simulated A-scan signal

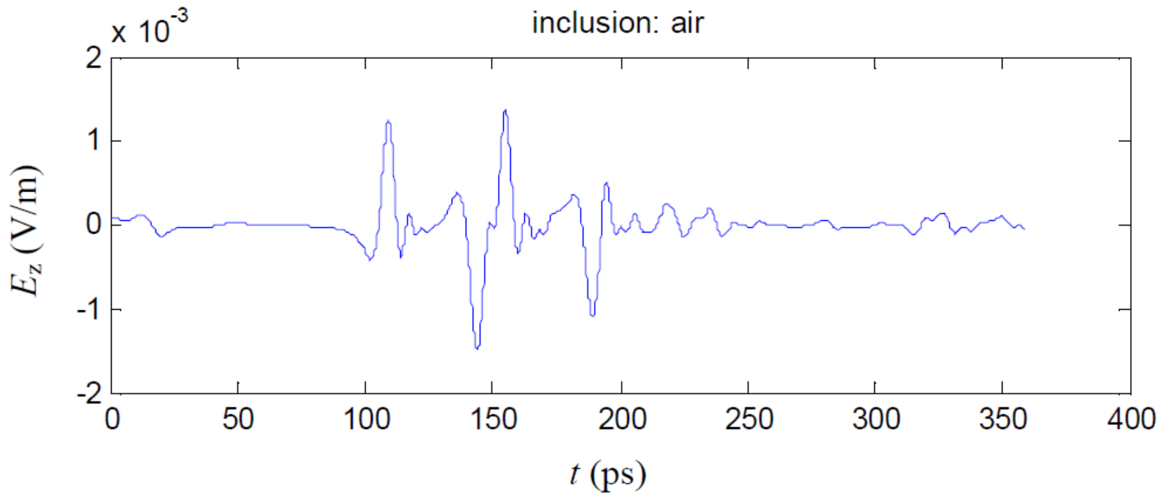

measured A-scan signal

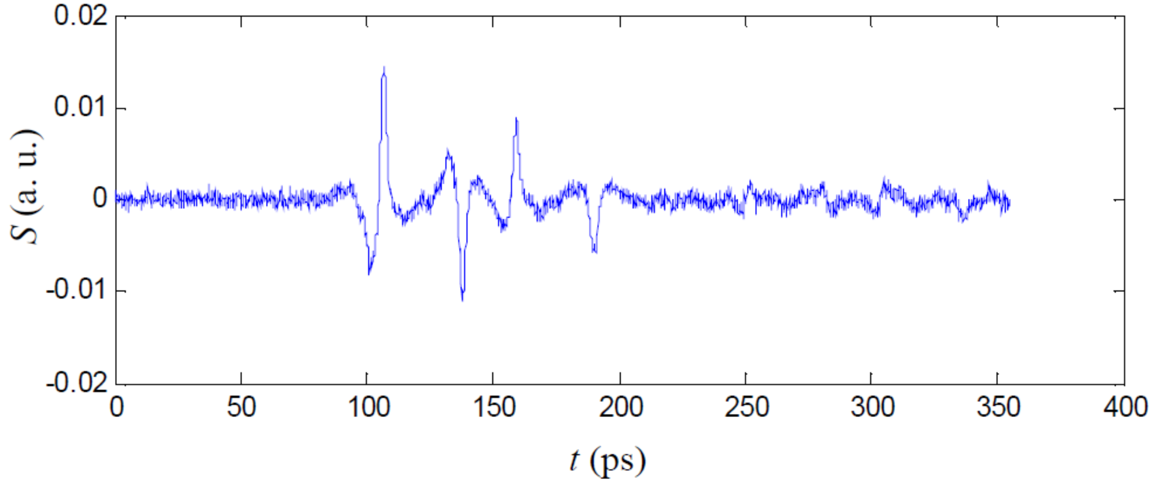

Summary

- We presented full-wave analysis of pulsed terahertz NDT system:
  - in frequency domain using FEM,
  - in time domain using FDTD.
- Despite the limitations associated with the demand for computing power, developed models allow a broad analysis of pulsed terahertz flaw detection systems.
- Comparison of A-scan signal calculated using simple FDTD model and measured one seems to be promising, especially for such simple evaluated structures as presented.
- Despite neglecting the influence of absorption and dispersion, the model can be used for computer-aided design of geometry of the measuring system or the development of dedicated terahertz signal processing algorithms.

Thank you

Questions….. ?